


ORIGINAL ARTICLE

The anti-wrinkles properties of sodium acetylated hyaluronate

Marie Meunier MS¹  | Amandine Scandolera PhD¹ | Emilie Chapuis BS¹ |
Laura Lapierre BS¹ | Jérôme Sandré MD² | Gerhard Brunner PhD³ |
Martin Lovchik PhD³ | Romain Reynaud MS⁴

¹Givaudan Active Beauty, Research and Development, Pomacle, France

²Polyclinique Courlancy, Reims, France

³Givaudan Suisse SA, Dubendorf, Switzerland

⁴Givaudan Active Beauty, Research and Development, Toulouse, France

Correspondence

Marie Meunier, Givaudan Active Beauty, Route de Bazancourt, 51110 Pomacle, France.

Email: marie.meunier@givaudan.com

Abstract

Background: Intrinsic aging promotes wrinkles formation by an imbalance between matrix synthesis/degradation in favor of degradation. This is accelerated by the exposure leading to overproduction of protease and fewer remodeling.

Objective: Protecting the integrity of extracellular matrix appears as the most efficient anti-aging solution. We developed a grafted HA specifically designed to get anti-aging property due to a specific molecular weight and acetylation degree.

Methods: A transcriptomic analysis was performed on fibroblasts, followed by a measurement of MMP secretion and subsequent effect on collagen degradation. MMP expression in skin explants concerned by chronobiological and extrinsic aging was analyzed by immunostaining. A clinical study was conducted on volunteers presenting wrinkles on face to evaluate flash reduction of wrinkles after 6 h of application by profilometry and anti-aging efficacy after 2 months by VISIA[®] CR2.3.

Results: Transcriptomic analysis evidenced an inhibition of MMP gene expression with acetylated HA, confirmed by an inhibition of MMPs release by fibroblasts, and a protection of type I collagen against degradation. We confirmed the reduction of MMPs in mature skin and in skin explants exposed to UV and urban dust. We demonstrated during clinical studies the flash reduction effect of acetylated HA on crow's feet wrinkles and a filling of nasogenian areas 6 h after application, and a wrinkles number reduction on nasogenian area up to 2 months of application.

Conclusion: We developed a new grafted HA owing protective properties against ECM degradation induced by chronobiological and extrinsic aging, leading to a significant and efficient anti-wrinkles effect.

KEYWORDS

anti-wrinkles, extracellular-matrix, extrinsic aging, intrinsic aging, sodium acetylated hyaluronate

This is an open access article under the terms of the [Creative Commons Attribution-NonCommercial-NoDerivs](https://creativecommons.org/licenses/by-nc-nd/4.0/) License, which permits use and distribution in any medium, provided the original work is properly cited, the use is non-commercial and no modifications or adaptations are made.

© 2021 The Authors. *Journal of Cosmetic Dermatology* published by Wiley Periodicals LLC.

1 | INTRODUCTION

The skin is composed of three distinct layers: from the surface down, the epidermis, dermis, and hypodermis.¹ Each layer has its own composition, which is associated with its specific role in the skin. The epidermis, composed of several layers of keratinocytes, is the outermost layer of the skin and is exposed to external factors but is continually renewed to overcome the potential degradation induced by these factors.^{2,3} The innermost layer, the hypodermis, is made of large pockets of adipose tissue whose main role is to isolate and protect the skin from shocks.¹ Between these layers is the dermis, a highly vascularized tissue mainly composed of fibroblasts, which synthesize structural proteins such as collagens, proteoglycans, and elastin.^{4,5} Type I and type III collagens, the two main types of collagens synthesized in the dermis, are arranged in a triple helix to form collagen fibers. These fibers are arranged perpendicularly to the epidermis and are intertwined with thin vertical oxytalan and elaunin fibers, which are poor in elastin and rich in fibrillin, in the papillary dermis. However, they are arranged parallel to the epidermis and are associated with thicker horizontal mature elastic fibers enriched in elastin in the underlying reticular dermis.⁶ These different organizational types in the papillary and reticular dermis confer firmness but also strong elastic properties to the skin.^{7,8} These fibers are associated with other structural proteins, such as type V collagen, hyaluronate, and many other molecules, thus forming the extracellular matrix (ECM) which constitutes a scaffold for the skin.^{4,9}

During intrinsic aging, an imbalance occurs between the synthesis and degradation of these macromolecules, owing to their slow turnover associated with their long half-life.¹⁰ Aging fibroblasts synthesize more prostaglandin E2 (PGE2), an inhibitor of collagen production, and thus progressively lose their ability to synthesize collagen.^{11,12} Moreover, matrix metalloproteinases (MMPs) accumulate during aging, thereby increasing collagen degradation.¹³ The accumulated MMPs associated with aging include collagenases (MMP-1), stromelysins (MMP-3), and gelatinases (MMP-9). MMP-1 is the most efficient protease in initiating fragmentation of type I and type III collagen fibers by cleaving the triple helix. Collagen fragments are then degraded by MMP-3 and MMP-9.¹⁴

Skin aging can be accelerated by the exposome, comprising the external factors to which the skin is exposed daily, including UV radiation, pollution, tobacco, and blue light. These various exposures increase the production of reactive oxygen species (ROS), thus resulting in deleterious effects on the skin and leading to premature aging, commonly referred to extrinsic aging.^{15,16} Studies have clearly shown that the production of ROS by UV radiation indirectly stimulates the synthesis of MMPs.¹⁷ Indeed, ROS activate MAP kinases, which in turn induce the expression of c-Fos and c-Jun, whose association forms the transcription factor activator protein 1 (AP-1), thereby triggering the overexpression of genes encoding MMP-1, MMP-3, and MMP-9.¹⁷ Moreover, AP-1 decreases the production of pro-collagen type I production by fibroblasts through inhibiting

the transforming growth factor- β (TGF- β) pathway.¹⁸ Similarly to UV radiation, ozone pollution has severe consequences on the skin, because it stimulates MMP-9 gene expression and activity, and consequently enhances collagen degradation in the dermis.¹⁹ Data from the literature have confirmed that the exposome can induce premature aging through increasing the expression and activity of MMPs, which are naturally stimulated by intrinsic aging.

Alterations of collagens from the ECM, through the inhibition of their synthesis and the stimulation of their degradation, are responsible for the dermis thinning, thereby leading to clinical manifestations such as the formation of wrinkles. Consequently, protecting the ECM against degradation through MMP inhibition and the introduction of an external source of ECM in the skin appears to be an efficient anti-aging strategy.²⁰ Among potential external sources of ECM that may provide anti-aging solutions, hyaluronic acid (HA) is one of the best known and renowned.

HA is an iconic cosmetic active ingredient, owing to its multiple physiological roles in promoting hydration, and improving viscoelasticity and tonicity by creating a hydrogel in the ECM. First generation HA has a high molecular weight of approximately 1 million Daltons and mainly has skin surface effects including high moisturization.²¹ Hydrolyzed HA (second generation) with intermediate and lower molecular weights was subsequently developed to improve skin penetration and provide additional biological activities.²² The skin penetration of HA varies according to the molecular weight.²³ We have demonstrated that high molecular weight HA remains at the surface of the skin, whereas HA with intermediate (300 kDa) and low (20–50 kDa) molecular weights penetrates deeper into the skin, up to 120 μm for the lowest molecular weight. Intermediate and low molecular weight HA trigger numerous biological pathways including cell proliferation, migration, cell communication, and microbial defense.^{22,24} These mechanisms are triggered after HA interacts with the natural receptor CD44 and by interaction with Toll-like receptors, such as TLR2 or TLR4, which induce microbial defense through the production of beta-defensin.²²

These two forms of HA, native and hydrolyzed, confer transient skin benefits, because the skin is enriched in hyaluronidase, which degrades HA. During aging, expression of this enzyme increases,²¹ thus increasing the degradation of natural HA and limiting the long-lasting effect of exogenous HA.

Extending this knowledge, we developed a new anti-aging solution based on a grafted HA, which is able to penetrate into the skin, has biological activity, and is resistant to hyaluronidase. Using a particular range of molecular weight and acetyl grafts, we demonstrated that the acetylation of HA promotes high resistance to hyaluronidase and deep penetration in the skin. Then, we demonstrated through *in vitro* and *ex vivo* studies that this acetylated sodium hyaluronate has beneficial effects in protecting the ECM against the degradation associated with intrinsic and extrinsic aging. Finally, we confirmed by clinical studies that this ECM protection leads to a strong and visible anti-wrinkle effect.

2 | METHOD

2.1 | Raw material

HA with a specification of molecular weight between 20 and 50 kDa (Mn) was used as the starting material and was fully acetylated. Native sodium hyaluronate was obtained by fermentation processes. Then, it has been fully acetylated thanks to green biochemistry processes as described in the following patent (WO2018/162672A1). We obtained a fully acetylated final product with an average molecular weight of 15 kDa (Mn). We compared the efficiency of this acetylated product to a non-acetylated form with an equivalent molecular weight (15 kDa Mn).

2.2 | Skin penetration with Raman spectroscopy

The analysis was performed on frozen skin explant from Caucasian donors (mean age of 36 ± 1). Skin explants were topically treated with sodium acetylated hyaluronate at 1% (w/v) or sodium hyaluronate at 1% (w/v) which are same molecular weight (15 kDa) and were then incubated for 8 h at 32°C. The untreated skin explant was used as a negative control. After the incubation phase (T8 h), the surfaces of the explants were cleaned to eliminate any excess product.

The explants were frozen at -80°C and then cut longitudinally with a Cryotome (MICROM HM 500 OM., MICROM International GmbH) to a thickness of 20 μm . For each explant, three tissue sections were selected and deposited on a CaF2 support for Raman imaging analysis.

Raman spectral acquisitions were recorded by using a Labram microspectrometer (Horiba Jobin Yvon) associated with a microscope (BX40; Olympus) coupled to a dispersive Raman spectrograph. The complete and detailed information regarding the method was described by Essendoubi et al.²³

The Raman images had a size of Y: 10 μm /X: 100 μm with a step of 5 μm in X and 5 μm in Y. Each Raman image had 3 Y spectra and 21 X spectra (63 spectra per image).

2.3 | Resistance to hyaluronidase

Sodium acetylated hyaluronate and sodium hyaluronate which are same molecular weight (15 kDa) were prepared at 2% (w/v) in water and mixed for 5 min. Then, 300 μl of these solutions was placed in contact with hyaluronidase solution at 8 UI/ml, which was previously validated as the optimal concentration of hyaluronidase needed to induce sodium hyaluronate degradation in this *in tubo* model. The negative control involved a solution without hyaluronidase. All reactions were then mixed and incubated at 55°C in an oven for 16 h and then cooled to room temperature. HA was extracted via the mobile phase and centrifuged at 5600 g for 10 min. The molecular weight of each HA (acetylated and non-acetylated forms) was determined with chromatographic analysis, according to a confidential method performed by a subcontractor.

2.4 | Transcriptomic analysis of normal human fibroblasts

Normal human dermal fibroblasts (NHDFs) obtained from a donor who had an abdominal surgery under informed consent were seeded at 250 000 cells per well in 6-well plates. After 72 h of culture, the cells were stimulated for 24 h with sodium acetylated hyaluronate or with non-acetylated hyaluronate, which are same molecular weight (15 kDa) as a control at 0.01% (w/v) for NHDF in free Dulbecco's Modified Eagle's Medium (DMEM from Gibco, Thermo Fisher Scientific). After 24 h of treatment, RNA was extracted with the TRIzol method (Invitrogen, Thermo Fisher Scientific). RNA quality was controlled, and reverse transcription was performed to obtain cDNA. RT-qPCR was performed on pre-coated plates (Applied Biosystems) specifically designed to study the transcriptomic expression of genes involved in dermis function, extracellular matrix component, remodeling, antioxidant enzymes, stress defenses, cell proliferation, DNA repair, and stem cell markers (the detailed list of genes belongs to Givaudan and is maintained confidential) with 10 ng of cDNA per well, a CFX96 Touch system (Bio-Rad) and Universal TaqMan mix (Quanta). The results of gene expression were normalized to GADD45A (Growth Arrest And DNA Damage Inducible Alpha) housekeeping gene expression. All conditions were realized in triplicate.

2.5 | Inhibition of metalloproteinase expression in vitro

Normal human dermal fibroblasts freshly isolated from a skin biopsy were seeded in 12-well plates at 150 000 cells per well in complete medium composed of DMEM (Gibco, Thermo Fisher Scientific) and 1% (v/v) antibiotic (penicillin and streptomycin from Sigma). At confluence, the cells were washed with phosphate buffered (PBS, from Gibco, Thermo Fisher Scientific) and starved by fetal calf serum (Biowest) deprivation for 24 h in DMEM. Cells were pre-incubated with sodium acetylated or non-acetylated hyaluronate which are same molecular weight (15 kDa) at 0.01% (w/v) for 2 h at 37°C and were then exposed to oxidative stress (H_2O_2 200 μM , Sigma-Aldrich) for 2 h at 37°C or left unexposed. The culture medium was replaced by basal medium, and the cells were incubated for 48 h at 37°C. At 48 h after oxidative stress induction, conditioned medium was collected and stored at -20°C. Supernatants were then used to analyze the released MMP-1 and MMP-3 through Luminex analysis (Human MMP premixed Magnetic Luminex Performance Assay, Ref panel: 1307e319 [MMP-1, MMP-3], R&D Systems). All conditions were realized in triplicate.

2.6 | DQ-collagen degradation

Normal human dermal fibroblasts freshly isolated from a skin biopsy were seeded in 12-well plates at 150 000 cells per well in

complete medium composed of DMEM (Gibco, Thermo Fisher Scientific) and 1% ATB (penicillin and streptomycin, Sigma-Aldrich). At confluence, the cells were washed with PBS and starved by fetal calf serum (Biowest) deprivation for 24 h in DMEM. The cells were pre-incubated with sodium acetylated or non-acetylated hyaluronate which are same molecular weight (15 kDa) at 0.01% (w/v) for 2 h at 37°C and were then exposed to oxidative stress (H_2O_2 200 μ M, Sigma-Aldrich) for 2 h at 37°C or left unexposed. The culture medium was replaced by basal medium, and the cells were incubated for 48 h at 37°C. At 48 h after oxidative stress induction, conditioned medium was collected and stored at -20°C. Supernatants were then used to analyze the collagen degradation mediated by the active MMPs present in the samples, by using DQ-collagen (DQ™ collagen, type I F, 10562903, Invitrogen, Thermo Fisher Scientific). Briefly, 100 μ l of each sample was deposited in the corresponding wells. A mixture of reaction buffer containing 50 mM Tris-HCl, 0.15 M NaCl, 5 mM $CaCl_2$, and 0.2 mM sodium azide at pH 7.6 and the QD-collagen at 50 μ g/ml was prepared and added to each well. The plate was incubated 4 h at room temperature in the dark, and the emitted fluorescence corresponding to type I collagen degradation was measured with a Micro-plate Reader (TECAN) with the absorption maximum at 495 nm and fluorescence emission maximum at 515 nm. All conditions were realized in triplicate.

2.7 | Skin explant maintenance in culture for chronobiological aging analysis

The test was performed on NativeSkin® patented (US patent US9585381B2) mature skin explants (Genoskin), full-thickness skin biopsy samples. NativeSkin models® are embedded in a solid and nourishing matrix with the epidermal surface in contact with air. The skin biopsy is firmly embedded in the matrix, thereby preventing lateral diffusion of topically applied formulations. Animal component-free and xeno-free skin culture medium is renewed every day, allowing keeping skin biopsies alive until 7 days of culture. The product sodium acetylated hyaluronate was applied by topical application at 0.1%. The product was applied once per day for 5 days and compared with untreated skin explants.

2.8 | Metalloproteinase-1 (MMP-1) and metalloproteinase-9 (MMP-9) expression detected by immunohistochemistry in chronobiological aging skin explants

Skin explants were fixed in formalin (Sigma-Aldrich) for 24 h, dehydrated, embedded in paraffin, and sectioned. After an antigenic retrieval step, tissue sections were blocked with PBS containing 2% BSA for 1 h. The markers of interest were then detected by immunofluorescence analysis. Primary antibodies were incubated overnight at 4°C. Alexa fluor 594 secondary antibody (1/1000, Invitrogen,

Thermo Fisher Scientific) was incubated 1 h at room temperature. The biomarker expression was analyzed by fluorescence microscopy (DM5000B–Leica Microsystems), with ten images acquired for each of two biomarkers: MMP-1 (rabbit polyclonal antibody) and MMP-9 (rabbit polyclonal antibody). Fluorescence was quantified for each image through software imaging (Image J) in the dermis only. The region of interest was delimited; the total fluorescence intensity was calculated and then reported to the total area of interest. The specific labeling is gray, and the nuclei are blue, owing to DAPI staining (scale bars 100 μ m).

2.9 | Induction of extrinsic aging ex vivo (photo-pollution exposure)

Human skin explants were prepared on an abdominoplasty sample from mature Caucasian female. The explants were maintained in BEM culture medium (BIO-EC's Explants Medium, Laboratoire BIO-EC) at 37°C in a humid, 5% CO_2 atmosphere. On day 0 (D0), the product containing sodium acetylated hyaluronate at 0.1% (w/v) was topically applied at 2 μ l per cm^2 and spread with a small spatula. The "untreated" control explants did not receive any treatment except the refreshing of the culture medium. The culture medium was refreshed entirely (2 ml) on D1 after pollutants exposure. The outdoor pollutants comprised heavy metals and hydrocarbon (Table 1) together with UV exposure. On D1, 24 h after treatment with the tested products, the explants were placed on a PolluBox® system (Laboratoire BIO-EC) with 900 μ l per well of HBSS (Gibco, Thermo Fisher Scientific) and exposed by vaporization to a mixture of hydrocarbons plus heavy metals supplemented with NaCl 0.9% (150 μ l of NaCl 0.9% per ml of pollutant solution) for 1.5 h. After the pollutant exposure, the explants received UVA irradiation at a dose of 13.5 J/ cm^2 (3 minimal erythema dose, MED) by using a Vilbert Lourmat simulator RMX 3 W. In parallel, the unexposed explants were placed outside the incubator in a 12-well plate with 1 ml HBSS per well, in the dark and without exposure to pollution. At the end of the exposure, all explants were returned to the incubator under standard culture conditions in 2 ml of fresh BEMc per well.

2.10 | Metalloproteinase (MMP-1 and MMP-9) expression in skin explant exposure to extrinsic aging

MMP-1 immunostaining was performed on paraffin treated sections with a monoclonal anti-MMP-1 antibody (MAB901, R&D systems) diluted at 1:25 in PBS, 0.3% BSA and 0.05% Tween 20, incubated for 1 h at room temperature, with a Vectastain Kit Vector amplifier avidin/biotin system (Vector Laboratories). Visualization was performed with VIP, a substrate of peroxidase (Vector SK-4600, Vector Laboratories). The staining was performed with an automated slide-processing system (Dako, AutostainerPlus, Agilent Technologies) and was assessed through microscopy observation. The signal was quantified in the epidermis and dermis.

TABLE 1 Detailed composition of the pollutant solution used in the extrinsic aging ex vivo model

Heavy metals	Concentration	Hydrocarbons	Concentration
Al	0.01 mg/ml	Benzene	1 µl/ml
AS	0.01 mg/ml	Xylene	1 µl/ml
B	0.001 mg/ml	Toluene	1 µl/ml
Ba	0.001 mg/ml	—	—
Be	0.0005 mg/ml	—	—
Ca	0.005 mg/ml	—	—
Cd	0.001 mg/ml	—	—
Cr	0.001 mg/ml	—	—
Cu	0.001 mg/ml	—	—
Fe	0.001 mg/ml	—	—
Hg	0.0025 mg/ml	—	—
K	0.0495 mg/ml	—	—
Li	0.001 mg/ml	—	—
Mg	0.0005 mg/ml	—	—
Mn	0.0005 mg/ml	—	—
Na	0.01 mg/ml	—	—
Ni	0.0025 mg/ml	—	—
P	0.005 mg/ml	—	—
Pb	0.01 mg/ml	—	—
Sc	0.0005 mg/ml	—	—
Sa	0.01 mg/ml	—	—
Sr	0.0005 mg/ml	—	—
Te	0.01 mg/ml	—	—
Ti	0.001 mg/ml	—	—
Y	0.0005 mg/ml	—	—
Zn	0.001 mg/ml	—	—

MMP-9 immunostaining was performed on frozen sections with a polyclonal anti-MMP-9 antibody (NB600-1217, Novus Biologicals) diluted at 1:400 in PBS, 0.3% BSA and 0.05% Tween 20, and incubated for 1 h at room temperature. Detection was performed with Alexa Fluor 488 (A11008, Life Technologies, Thermo Fisher Scientific). The nuclei were counter-stained with propidium iodide. The staining was performed with an automated slide-processing system (Dako, AutostainerPlus, Agilent Technologies) and was assessed through microscopy observation. The signal was quantified in the epidermis and the dermis.

2.11 | INCI formula used in clinical study

The INCI formula was as follows: AQUA/WATER, ± SODIUM ACETYLATED HYALURONATE, CAPRIC/CAPRYLIC TRIGLYCERIDE, CETEARYL WHEAT STRAW GLYCOSIDES, CETEARYL ALCOHOL, PHENOXYETHANOL, METHYL PARABEN, PROPYL PARABEN, ETHYL PARABEN, DIMETHICONE, FRAGRANCE, HEXYL CINNAMAL, BUTYLPHENYL METHYLPROPIONAL, CITRONELLOL,

ALPHA ISOMETHYL IONONE, HYDROXYISOHEXYL 3-CYCLOHEXENE CARBOXALDEHYDE SODIUM HYDROXIDE.

2.12 | Panel description of the flash reduction of wrinkles on crow's feet and the nasogenian area

A double-blind, placebo-controlled clinical evaluation was performed on 21 volunteers (women 42 to 70 years old, with a mean age of 63 ± 2.16) who had crow's feet and nasolabial wrinkles. All participants provided signed informed consent at the beginning of the study. The study was conducted according to the guidelines of the Declaration of Helsinki. This study performed on cosmetic products coming within the definition of article L. 5131-1 of the French Public Health Code is in accordance with Decree n° 2017-884 of May 9, 2017, modifying some regulatory requirements concerning researches involving human subjects.

The cream containing the active ingredient was compared with the placebo during this study. The volunteers applied the products on half their faces at D0, and the flash anti-aging efficacy was measured with profilometry and VISIA® CR2.3 analysis 6 h after application in comparison with D0. The active ingredient was tested at 0.2% in this study.

2.13 | Panel description of the wrinkle reduction in the nasogenian area after 1 month of application

A double-blind, placebo-controlled clinical evaluation was performed on 20 volunteers (women 35 to 70 years old, with a mean age of 56 ± 6.69) with nasolabial wrinkles. All participants provided signed informed consent at the beginning of the study. The study was conducted according to the guidelines of the Declaration of Helsinki. This study performed on cosmetic products coming within the definition of article L. 5131-1 of the French Public Health Code is in accordance with Decree n° 2017-884 of May 9, 2017, modifying some regulatory requirements concerning researches involving human subjects.

The cream containing the active ingredient was compared with the placebo during this study. The volunteers applied the products twice daily on half their faces for 1 month (morning and evening). The anti-aging efficacy was measured with VISIA® CR2.3 analysis after D0 and 28 days (D28) of application. The active ingredient was tested at 0.1% in this study.

2.14 | Panel description of the wrinkle reduction in the nasogenian area after 2 months of application

A double-blind, placebo-controlled clinical evaluation was performed on 30 volunteers (women 50 to 70 years old, with a mean age of 57 ± 9) with wrinkles on their faces. All participants provided signed informed consent at the beginning of the study. The study was conducted according to the guidelines of the Declaration of

Helsinki. This study performed on cosmetic products coming within the definition of article L. 5131-1 of the French Public Health Code is in accordance with Decree n° 2017-884 of May 9, 2017, modifying some regulatory requirements concerning researches involving human subjects.

The cream containing the active ingredient was compared with the placebo during this study. The volunteers applied the products twice daily on half their faces during 2 months (morning and evening). Skin texture was measured with VISIA® CR2.3 analysis after

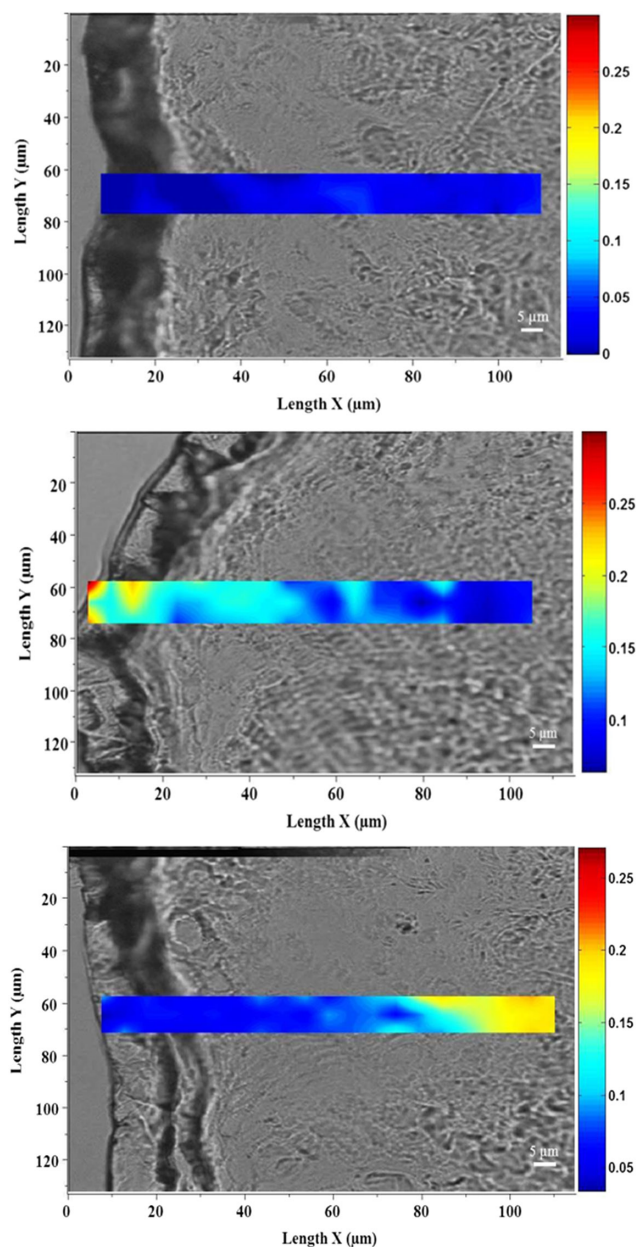


FIGURE 1 Impact of acetylation on the skin penetration of hyaluronic acid using Raman spectroscopy analysis. Frozen human skin explants were topically treated with nothing used as negative control in order to determine the Raman signal background related to the skin (top panel), 1% of hyaluronic acid (middle panel) or 1% of acetylated hyaluronic acid (bottom panel) which are same molecular weight (15 kDa) for 8 h before the Raman analysis

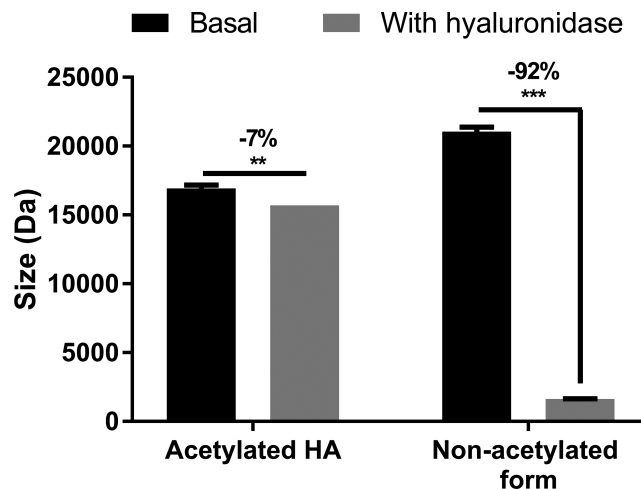


FIGURE 2 Effect of hyaluronidase activity on acetylated hyaluronic acid comparatively to without acetylation using in tubo assay. Acetylated hyaluronic acid and non-acetylated one which are same molecular weight (15 kDa) were put in contact at 2% with hyaluronidase enzyme for 16 h at 55°C. The enzymatic activity of hyaluronidase was indirectly measured by the detection of molecular weight of each tested HAs using HPLC profile analysis. The histogram represents the molecular weight in Da \pm SEM before and after contact with hyaluronidase. We used Student's *t*-test to do statistical analysis with ** $p < 0.01$, *** $p < 0.001$

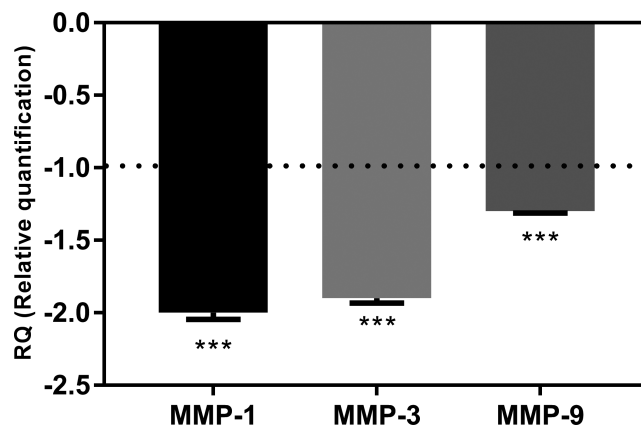


FIGURE 3 Representation of genes specifically regulated by sodium acetylated hyaluronate in comparison with non-acetylated form which are same molecular weight (15 kDa) and untreated condition, expressed in relative quantification \pm SEM. Normal human fibroblasts were incubated with active ingredient for 24 h, and gene expression analysis was done using real-time qPCR through TaqMan card. A statistical analysis was performed using Student's *t*-test with *** $p < 0.001$.

D0 and 56 days (D28) of application. The active ingredient was tested at 0.1% in this study.

2.15 | Crow's feet wrinkle analysis by profilometry

QUANTIRIDES® software (Monaderm) was used to analyze, quantify, and characterize the wrinkles of silicone resin impressions

(SILFLO). A negative replica of the wrinkles on the cutaneous surface was illuminated by a grazing light (35°), thus generating shadows behind each wrinkle. The image acquisition of these shadows was achieved with an IEEE high-resolution digital camera (XCD-SX910 camera, Sony). The QUANTIRIDES® software was used to analyze the images obtained and determine the characteristics of the wrinkles (surface, length, and depth). An area of 1.4 cm² was examined.

The studied parameters were the total wrinkled surface, the number and average depth of the micro-relief wrinkles, average wrinkles, and deep wrinkles.

Micro-relief wrinkles have a depth less than 55 µm. Average wrinkles have a depth between 55 and 110 µm, and deep wrinkles have a depth greater than 110 µm (up to 800 µm).

We also studied the number and the average length of the grooves for micro-relief wrinkles from 0 to 0.5 mm, average wrinkles from 0.5 to 2 mm, and deep wrinkles from 2 to 10 mm. Silicone polymer replicas of the crow's feet of volunteers were generated before use of the product and for each control performed during the study.

2.16 | Nasogenian wrinkles and skin texture analysis by VISIA® CR2.3

VISIA® tool has become a standard tool for diagnosis and analysis of skin in dermocosmetic research, thanks to the generation of photographs using standard, ultraviolet, and polarized lighting. Flash lighting allows identifying spots, wrinkles, texture, pore size, acne scars, brown spots, and many other skin parameters and characteristics.²⁵⁻²⁷ With VISIA® CR2.3, digital photographs of the face were collected at D0, T+1 h, T+6 h and after D28 and D56. Three types of photographs were acquired: right and left profiles and full face. VISIA® CR2.3 was used to study the nasogenian wrinkles after T1 h, T6 h, and D28, including the number, total area, and medium lines. We also used VISIA® CR2.3 analysis to study the skin texture after D56. VAESTRO software (Canfield Scientific) was used to analyze following parameters: "wrinkles analysis" with "count," "total area" and "area 3-medium lines."

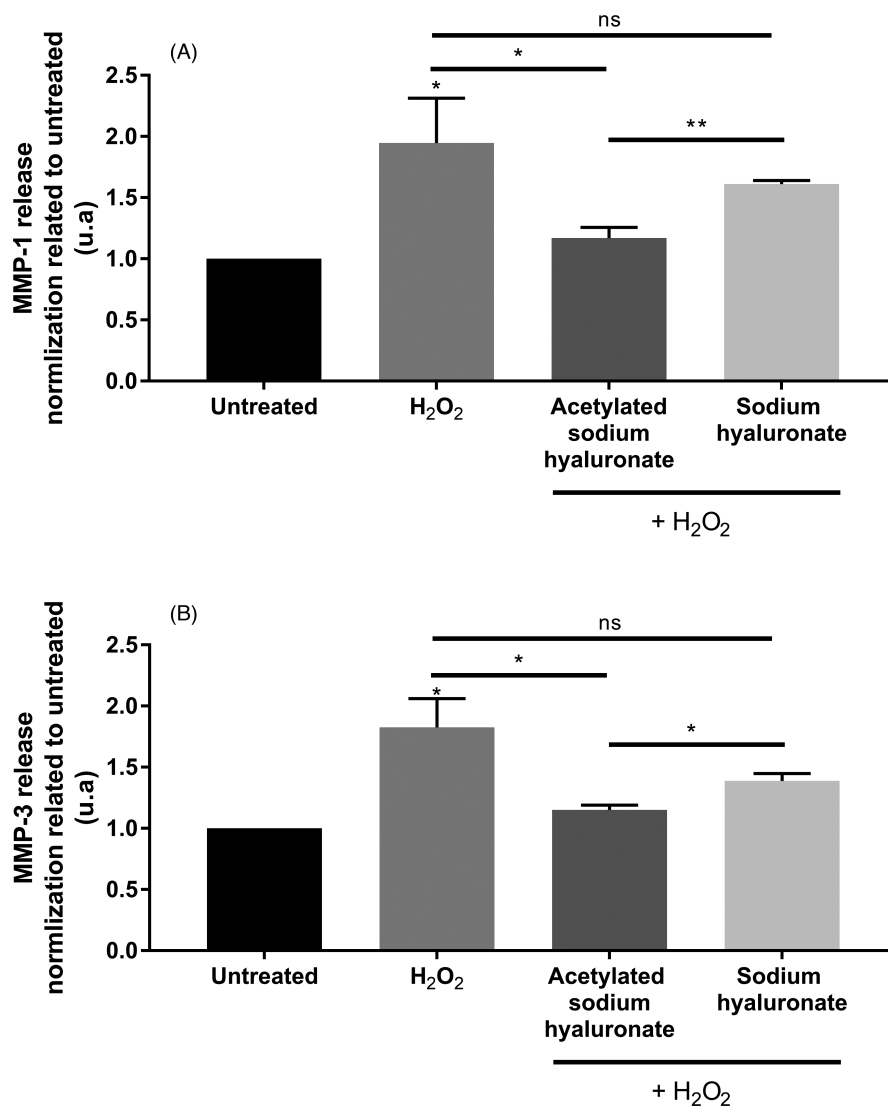


FIGURE 4 Inhibition of MMP-1 (A) and MMP-3 (B) release in normal dermal fibroblasts after premature aging induced by H₂O₂. Cells were pre-incubated with 0.01% of sodium acetylated hyaluronate or non-acetylated form which are same molecular weight (15 kDa) for 2 h before the induction of cell senescence which has been done by the addition of H₂O₂ at 200 µM for 2 h. Then, culture medium was renewed and the MMPs production was quantified after 48h of incubation. MMP-1 and MMP-3 secretion in supernatant was analyzed by ELISA performed with multiplex system and expressed according to untreated condition normalized at 1.0 ± SEM. We performed statistical analysis using Student's *t*-test with **p* < 0.05, ***p* < 0.01

2.17 | Statistical analysis

All results are presented as mean \pm standard error of the mean (SEM) of three independent triplicates. A Shapiro-Wilk test was used to verify whether the raw data followed the Gaussian law. In the case of normally distributed data, the mean values were compared using either an unpaired *t*-test. In the case of non-normally distributed data, a Kruskal-Wallis test followed by a Mann-Whitney U test was used for unpaired data. In all cases, results were considered as significant when $p < 0.1$ with #, $p < 0.05$ with *, $p < 0.01$ with ** and $p < 0.001$ with ***.

3 | RESULTS

3.1 | Improvements in skin penetration and long-lastingness

In the skin, HA is subjected to degradation by hyaluronidases, whose enzymatic activity increases with aging. As a consequence, an important loss of skin hydration and the formation of wrinkles occur with age.²⁸ We hypothesized that the acetylation of HA might improve its skin penetration and its bioavailability, thus providing an efficient anti-aging cosmetic solution. Using Raman spectroscopy analysis, we showed that the acetylation of HA substantially improved its skin penetration. Indeed, we demonstrated that non-acetylated HA was able to penetrate to 50 μm , whereas acetylated HA penetrated deeper, on the basis of Raman detection to 100 μm (Figure 1). In addition, hyaluronidase sensitivity analysis through *in tubo* assays

demonstrated that non-acetylated HA was almost entirely degraded by hyaluronidase: A 92% decrease in its molecular weight was observed. Under the same experimental conditions, the acetylation protected the HA against hyaluronidase activity, as demonstrated by the low degradation of -7% (Figure 2). Zhong et al. have used chemically modified HA to control its delivery and bioactivity, and have shown that some modifications, such as ethyl and benzyl esters, can protect against hyaluronidase activity. Moreover, they have suggested that the carboxyl groups in the β -glucuronic acid unit may be involved in hyaluronidase activity, and chemical modification of these groups restricts the cleavage of HA into smaller polymers.²⁹ Therefore, we presumed that the full acetylation of HA restricts access to the active site of hyaluronidase, thus leading to protection. Consequently, we demonstrated that the acetylation of HA improved its ability to penetrate into the skin and prolonged its lifespan.

3.2 | Properties against intrinsic aging

To determine whether the acetylation of HA might confer additional or new biological activities, we performed transcriptomic screening using a TaqMan array card targeting dermis function, including genes involved in matrix remodeling, extracellular components, dermal matrix degradation and synthesis, and antioxidant defense. We performed a comparative analysis of the gene expression profiles induced by normal HA and obtained by acetylated HA after 24 h of incubation at 0.01% on normal human fibroblasts. We identified protection against ECM degradation, owing to the down-regulation of expression of genes such as MMP-1, MMP-3, and MMP-9, with fold

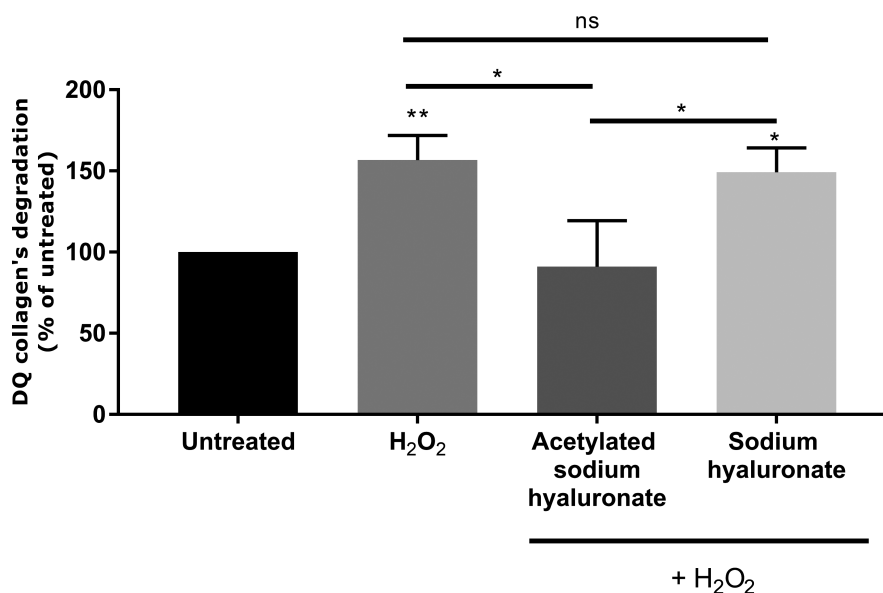


FIGURE 5 Degradation of type I collagen using DQ-collagen. Cells were pre-incubated with 0.01% of sodium acetylated hyaluronate or non-acetylated form which are same molecular weight (15 kDa) for 2 h before the induction of cell senescence, which has been done by the addition of H₂O₂ at 200 μM for 2 h. After the culture medium was renewed and the culture medium collected after 48 h of incubation, it was put in contact with DQ-collagen. The emitted fluorescence which is correlated to collagen degradation was measured at the excitation wavelength 495 nm and detected at wavelength of 515 nm using a Micro-plate Reader (TECAN) and expressed in percentage of untreated condition \pm SEM. We used Student's *t*-test to do statistical analysis with * $p < 0.05$ and ** $p < 0.01$

changes of -2 , -1.9 , and -1.3 , respectively (Figure 3). Indeed, these metalloproteinases are involved in collagen degradation, particularly that of type I collagen, the main component of the dermal matrix. Collagen degradation leads to the collapse of the skin scaffold structure and promotes wrinkle formation. The expression and activity of these enzymes sharply increase with aging.¹³ In this preliminary investigation, we hypothesized that acetylated sodium hyaluronate would have strong anti-aging properties and particularly would decrease wrinkle formation through dermal matrix protection. Using human dermal fibroblasts, we analyzed the effects of cell senescence chemically induced by H_2O_2 on MMP production. We demonstrated that the induction of premature aging significantly increased MMP-1 and MMP-3 release (Figure 4A,B). Indeed, cell senescence is known to be induced by several methods such as successive primary cell replication or chemical agents such as H_2O_2 .^{30,31} In addition, the induction of premature aging by H_2O_2 reproduces biological

alterations, such as a strong increase in MMP production, similarly to our observations.³²

Pre-incubation with acetylated HA at 0.01% significantly inhibited MMP secretion in the culture medium. We demonstrated that non-acetylated HA in the same experimental conditions slightly decreased MMP-1 and MMP-3 production, but this effect was not significant. More interestingly, we showed that the efficacy of acetylated HA in inhibiting MMP release was significantly better than that observed with the non-acetylated form (Figure 4). This biological activity was associated with the acetylation, because it was not observed with non-acetylated HA. MMPs can be produced in active and inactive (proform) forms.³³ We confirmed that the product inhibited the active forms of these MMPs. MMP-1 is involved in type I collagen degradation, and MMP-3 cleaves already degraded type I collagen into smaller fragments.¹⁴ We used DQ-type I collagen, which emits fluorescence when it is degraded,

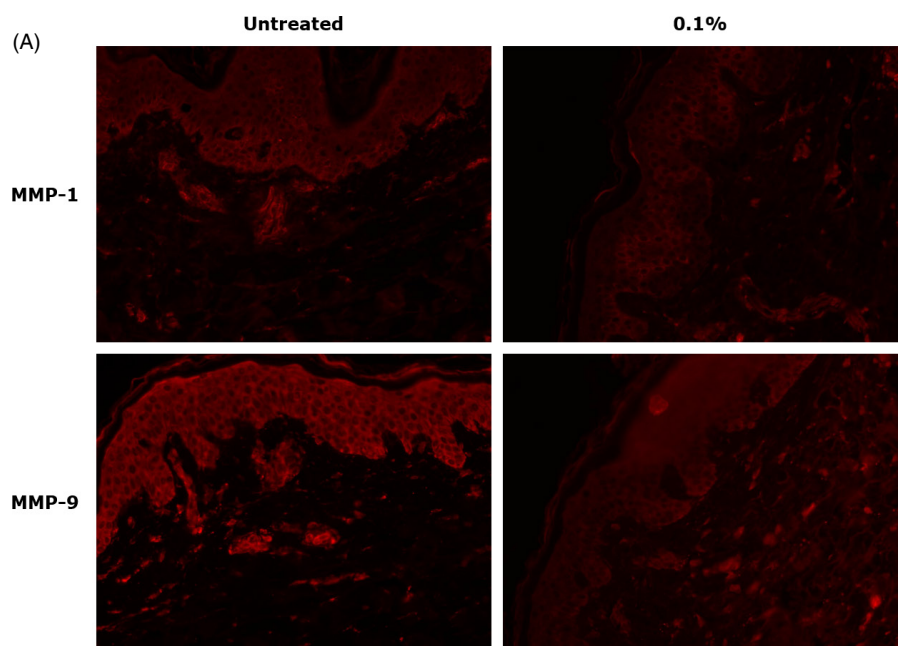
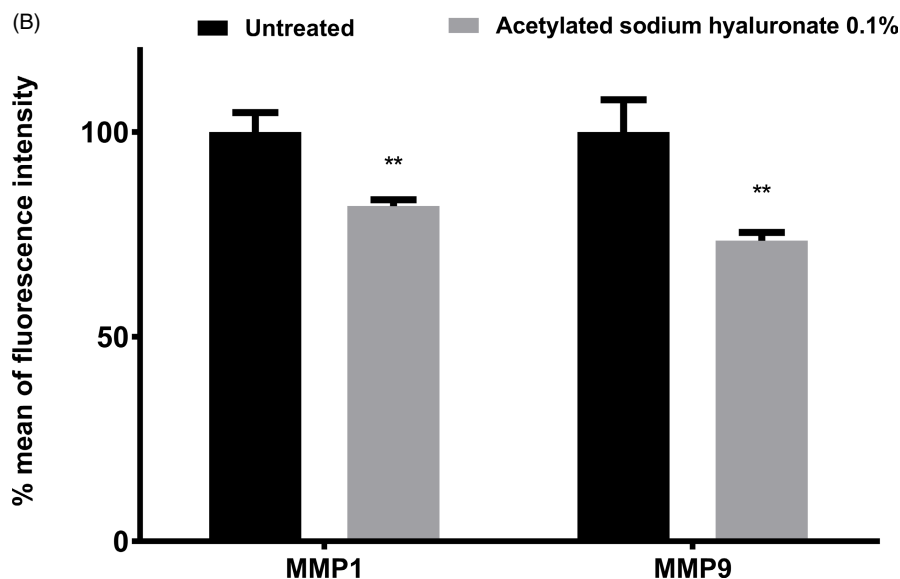


FIGURE 6 Impact of sodium acetylated hyaluronate on MMP-1 and MMP-9 expression during intrinsic aging using IHC. Skin explants were topically treated with sodium acetylated hyaluronate at 0.1% for 5 days and compared with untreated condition. The expression of MMP-1 and MMP-9 was then analyzed by specific immunostaining using specific primary antibodies anti-MMP-1 and MMP-9. Left panel represents illustrative pictures of MMP-1 and MMP-9 IHC, and right panel represents the quantification of the fluorescent signal in the dermis expressed in percentage of untreated condition \pm SEM. We used Student's *t*-test to do statistical analysis with $**p < 0.01$



through elimination of the bound quencher on the collagen by active MMPs. Our results demonstrated that premature aging induced by H_2O_2 treatment significantly increased type I collagen degradation, on the basis of the increased fluorescence, thus confirming the presence of active MMPs. Pre-incubation with acetylated

sodium hyaluronate significantly decreased collagen degradation, thus demonstrating the efficient protection of the collagen network through MMP inhibition. Moreover, this effect was specific to the acetylation, because the non-acetylated form did not have any effect and resulted in a significant increase in type I collagen degradation (Figure 5).

Thus, we demonstrated that acetylated sodium hyaluronate has anti-aging properties, particularly through protecting the dermal matrix from degradation by MMP inhibition. MMP-1 and MMP-3 are two main metalloproteinases that are over-expressed during aging and photo-aging.¹³ Indeed, they are integrally involved in wrinkle formation, owing to their roles in dermal scaffold degradation. Therefore, a disequilibrium exists between synthesis and matrix degradation in favor of degradation.¹⁰

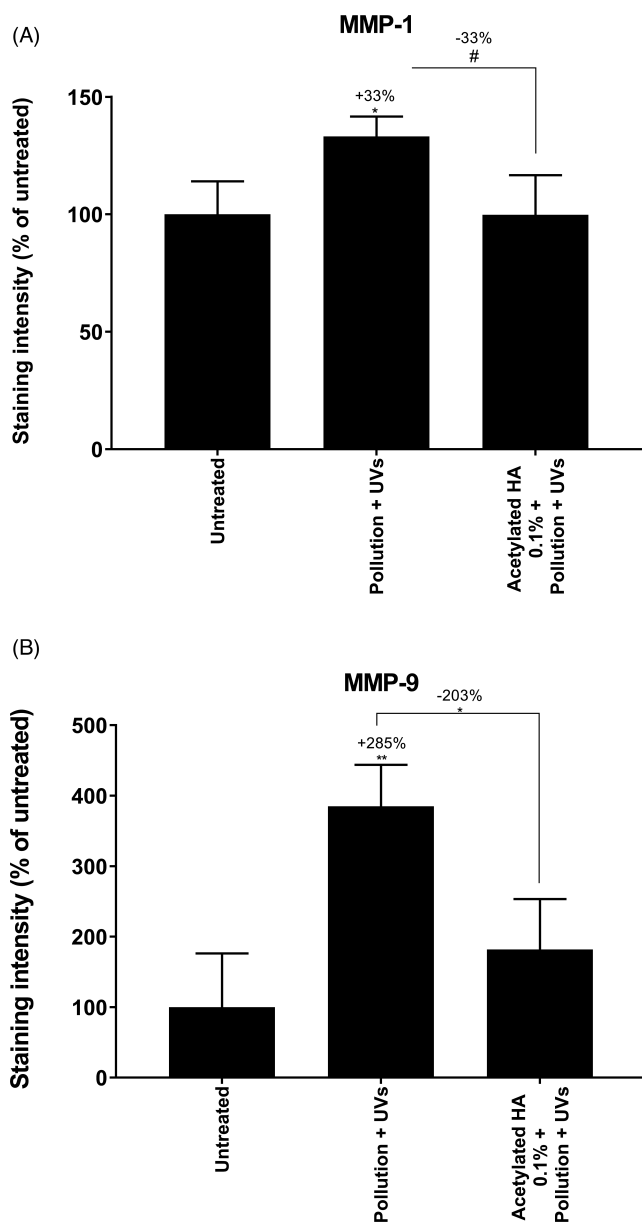


FIGURE 7 Impact of sodium acetylated hyaluronate on MMP-1 and MMP-9 expression during extrinsic aging induced by photo-pollution exposure. The extrinsic aging was mimicked by photo-pollution exposure on human skin explants. Skin explants were topically treated with sodium acetylated hyaluronate at 0.1% and compared with untreated condition. The expression of MMP-1 and MMP-9 were then analyzed by specific immunostaining using specific primary antibodies anti-MMP-1 and MMP-9. Left panel represents the quantification of MMP-1 expression relative to untreated condition, and right panel represents the quantification of MMP-9 expression relative to untreated condition in percentage \pm SEM. We used Student's *t*-test to do statistical analysis with # $p < 0.1$, * $p < 0.05$, ** $p < 0.01$

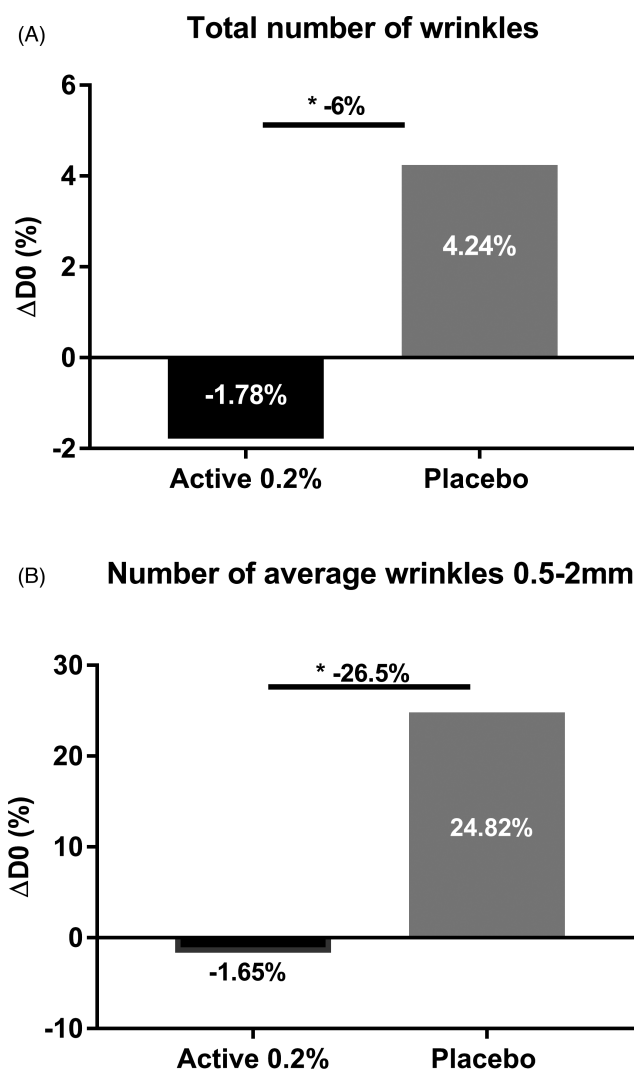


FIGURE 8 Impact of sodium acetylated hyaluronate at 0.2% formulated in cream versus placebo on total number of crow's feet wrinkles (A) and on the number of wrinkles between 0.5 and 2 mm (B) using profilometry measurement after 6 h of application. Data are expressed in mean of $\Delta D0_{6h} \pm$ SEM. Statistical analysis was performed by Student's *t*-test with * $p < 0.05$

3.3 | Properties against extrinsic aging

Overexpression of MMPs is observed during chronobiologic aging which is responsible for wrinkle formation, owing to excessive ECM degradation and the accumulation of ROS.¹³ Exposure to environmental factors such as UV, cigarette smoke and pollution exacerbates and accelerates skin aging by drastically increasing skin oxidation and MMP production, thus leading to premature aging with earlier formation of wrinkles.¹⁵ This phenomenon is called extrinsic aging. In this work, we sought to determine whether acetylated sodium hyaluronate might limit the over-expression of MMPs such as MMP-1 and MMP-9, which are involved in chronobiologic aging and extrinsic aging. First, we examined aged skin explants topically treated with acetylated sodium hyaluronate at 0.1%. Through specific immune-detection of MMP-1 and MMP-9, we demonstrated that acetylated sodium hyaluronate significantly decreased MMP-1 and MMP-9 expression in the dermis, thus confirming that this molecule prevents chronobiologic aging (Figure 6). To mimic extrinsic aging, we exposed skin explants to pollution by using urban dust vaporized in a Pollubox[®] combined with UV exposure. UV irradiation affects pollutant particles, thus resulting in deleterious synergistic effects on the skin.³⁴ We observed overexpression of both MMP-1 and MMP-9. MMP-9 in the dermis has very low expression in the basal layer and is known to be over-expressed in response to exposure components such as UV irradiation and ozone.^{19,35} Similarly, MMP-1, the most important MMP responsible for collagen destruction, is over-expressed in response to the exposome and is used as a biomarker of aging.¹⁷ In addition, the DNA damage after UV exposure leads to direct overproduction of MMP-1 in the skin.¹⁷ Finally, the overexpression of MMPs, particularly MMP-1 and MMP-9, may be interesting targets to prevent skin aging. During our investigations, we studied the effects of topical application of acetylated

sodium hyaluronate after photo-pollution exposure. Our data demonstrated that the topical application resulted in significantly lower expression of MMP-1 and MMP-9 than that in the untreated condition (−33% and −203%, respectively; Figure 7). The MMP expression after treatment was very close to that in the untreated condition, thus demonstrating that acetylated sodium hyaluronate has a protective effect against extrinsic aging induced by the exposome.

A decrease in MMPs, specifically their active forms, is now recognized as an efficient anti-aging strategy.²⁰ To validate this strategy, we conducted clinical studies to analyze the effects of acetylated sodium hyaluronate on wrinkle formation.

3.4 | Clinical anti-aging properties

We performed several clinical studies to demonstrate that the anti-aging property of sodium acetylated hyaluronate through protection against ECM degradation leads to an efficient decrease in wrinkles.

First, we evaluated the flash effect of sodium acetylated hyaluronate on crow's feet and nasogenian wrinkles in women. Using profilometry measurement based on silicone replica analysis on crow's feet wrinkles, we observed a slight decrease in the total number wrinkles 6 h after application, whereas the placebo showed an increased number. We further demonstrated a significant 6% lower total number of wrinkles with the active ingredient at 0.2% than with the placebo 6 h after application (Figure 8A). Specifically, we observed a significant effect on the average number of 0.5–2 mm wrinkles, which are considered medium lines; these were 26.5% fewer than those with the placebo (Figure 8B). On nasogenian wrinkles, we observed an 8% smaller coarse area than that with the placebo. Interestingly, we demonstrated that sodium acetylated hyaluronate at 0.2% decreased the coarse area of wrinkles, whereas the placebo increased this area 6 h after application (Figure 9). Throughout the day, skin fatigue occurs, thus increasing wrinkle number and depth.³⁶ Here, we confirmed at the clinical level that sodium acetylated hyaluronate, through its rapid penetration into the deep epidermis and resistance to hyaluronidase, provides a benefit on wrinkles by filling them. Thus, sodium acetylated hyaluronate preserved the initial state of the skin and limited the formation of wrinkles associated with skin fatigue, acting as a natural filler with a mechanical effect.

We performed a second clinical study to evaluate the effect of sodium acetylated hyaluronate at 0.1% on nasogenian wrinkles after 1 month of application. Our results showed that sodium acetylated hyaluronate at 0.1% significantly decreased the number and total area of nasogenian wrinkles, specifically medium lines, by 3.97%, 7.53%, and 11% with respect to D0 after 28 days of application. The placebo resulted in an opposite effect, with a slight increase in the number, total area, and medium lines after 28 days. Sodium acetylated hyaluronate, compared with the placebo, demonstrated significantly fewer nasogenian wrinkles (−9%), smaller total area (−12%), and medium lines (−13%) than those observed with the placebo after 28 days (Figure 10). The anti-aging effect can be visualized in illustrative pictures in Figure 10. We performed a third clinical study to

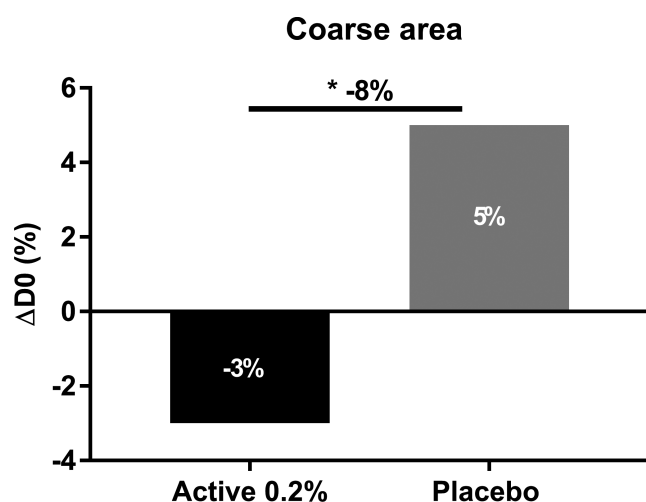


FIGURE 9 Impact of sodium acetylated hyaluronate at 0.2% formulated in cream versus placebo on the reduction of coarse area from nasogenian wrinkles after 6 h of application using VISIA[®] CR2.3 Analysis. Data are expressed in mean of $\Delta D0_{6h}$ (% \pm SEM). Student's t-test was used with * $p < 0.05$

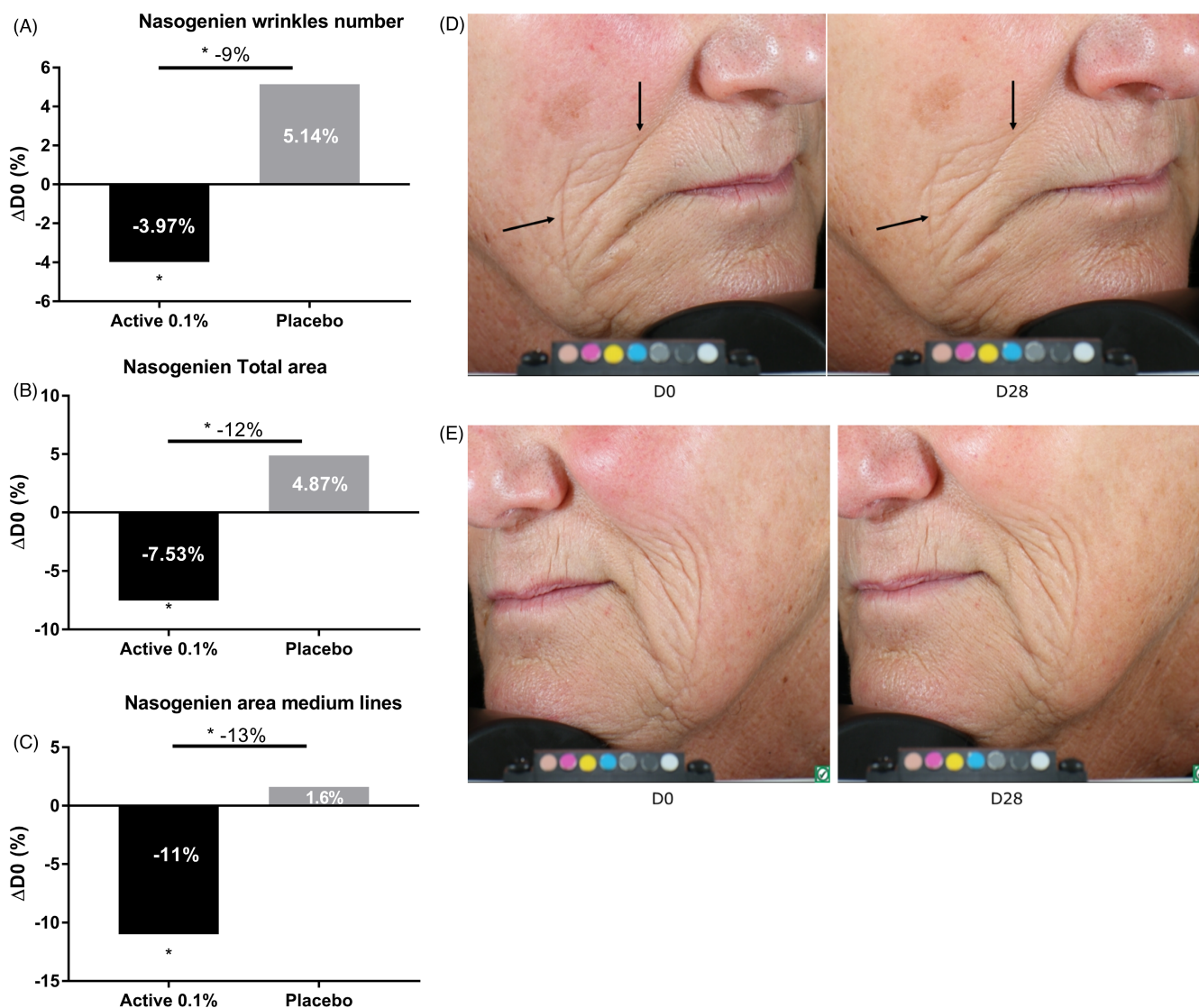


FIGURE 10 (A,B,C) Impact of sodium acetylated hyaluronate at 0.1% formulated in cream versus placebo on the reduction of coarse area from nasogenian wrinkles after 1 month of application using VISIA[®] CR2.3. Data are expressed in mean of $\Delta D0D28$ (% \pm SEM). Student's *t*-test was used for the statistical analysis with $*p < 0.05$. (D) Illustrative pictures showing the effect of sodium acetylated hyaluronate versus (E) Placebo

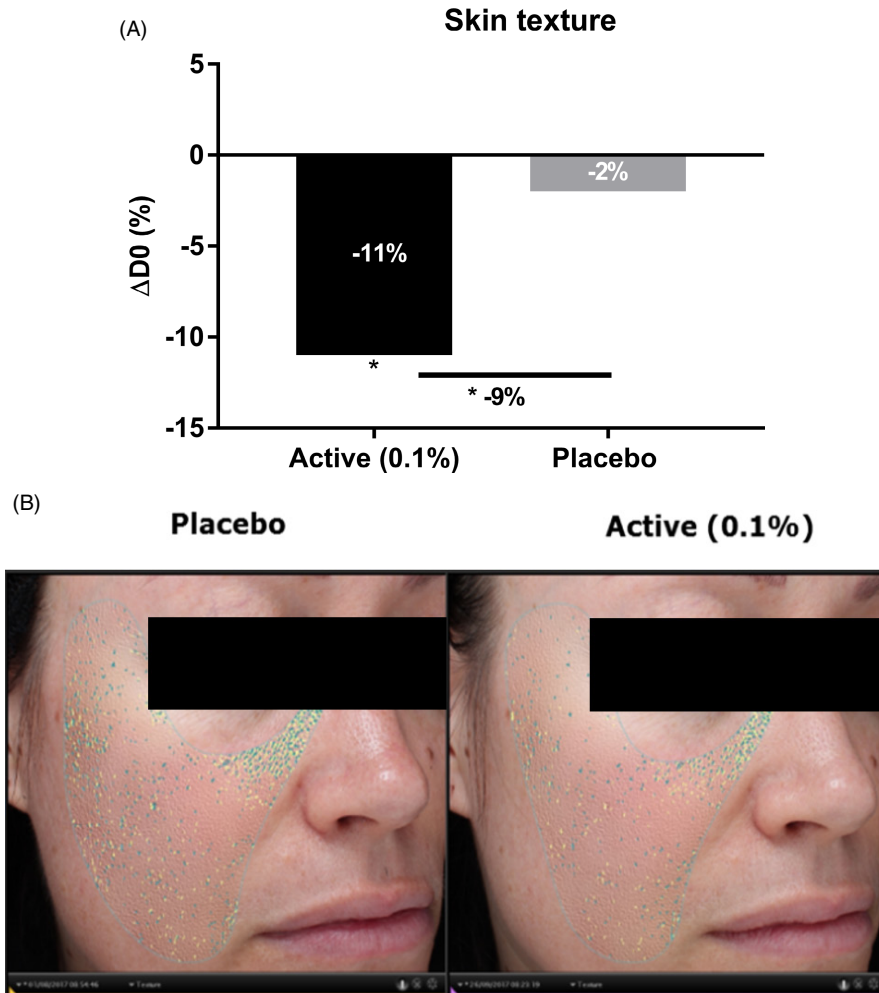
demonstrate the efficacy of sodium acetylated hyaluronate at 0.1% on skin texture. Indeed, the protection of the ECM network through the inhibition of its degradation improves skin structure and consequently wrinkles as previously demonstrated, but also has a smoothing effect. We then analyzed the effects of the active ingredient on skin texture after 2 months of application. We observed that sodium acetylated hyaluronate significantly decreased the roughness by 11% with respect to D0, whereas the placebo showed only a 2% decrease (Figure 11). In comparison with the placebo, the treatment significantly improved skin texture, with 9% less roughness relative to that with the placebo after 2 months of application. Together, these results demonstrated that sodium acetylated hyaluronate through protecting the ECM from degradation led to a decrease in

wrinkles. Therefore, protecting ECM integrity is a way to achieve efficient anti-aging activity.¹³

4 | CONCLUSION

In this study, we developed a new molecule derived from HA, sodium acetylated hyaluronate. We first demonstrated that the acetylation of HA provides protection against degradation by hyaluronidase, thus allowing for better and deeper penetration through the skin layers. During aging, the skin dermis undergoes damage, such as ECM component degradation, and this phenomenon is amplified by daily exposure to UV, pollution, and other external factors

FIGURE 11 Impact of sodium acetylated hyaluronate at 0.1% on skin texture after 2 months of application. Data are expressed in mean of $\Delta D0D56$ ($\% \pm$ SEM). Student's *t*-test was used for statistical analysis with $*p < 0.05$



that constitute the exposome. We presumed that the resistance of sodium acetylated hyaluronate to hyaluronidase and its deeper penetration in the skin would be an efficient way to protect the dermis against degradation. Indeed, we demonstrated *in vitro* that sodium acetylated hyaluronate, in comparison with the non-acetylated form, inhibits MMP gene expression and activity, thus decreasing collagen degradation. We confirmed this effect on skin explants, showing that sodium acetylated hyaluronate, through its deep penetration, decreases MMP expression in the dermis. Therefore, this active ingredient has the potential to protect the skin dermis against the degradation occurring during intrinsic aging. Furthermore, in skin explants exposed to UV and pollution, we observed that sodium acetylated hyaluronate also protects the skin dermis from the degradation that can be increased by the exposome. Our clinical investigations successfully highlighted sodium acetylated hyaluronate's protective effect on the skin dermis. Indeed, we showed a filling effect of the active ingredient 6 h after application on thin wrinkles in the crow's feet area, as well as efficacy in reducing deeper wrinkles in the nasogenian area and a smoothing effect regarding the skin texture after 28 days of treatment. Therefore, sodium acetylated hyaluronate has efficient anti-wrinkle activity through protecting ECM integrity.

ACKNOWLEDGEMENTS

A great thank to G. Brunner and M. Lovchik for their involvement in the development of sodium acetylated hyaluronate. We would like to thank J. Sandré and his team for his collaboration with Givaudan, allowing us working on fresh skin tissue and cells. We thank M. Meunier and A. Scandolera for their expertise in the management of *in vitro* and *ex vivo* studies. We also thank E. Chapuis and L. Lapierre for their expertise in the acquisition and analysis of clinical data. A. Scandolera and R. Reynaud are gratefully acknowledged for continuous support on this project and scientific discussions. The authors would like to thank Mohammed Essendoubi and Michel Manfait (Reims, France), Synelvia (Toulouse, France), Syntivia (Toulouse, France), BIO-EC (Longjumeau, France) for their great help in the completion of this paper.

AUTHORS' CONTRIBUTIONS

G.B. and M.L. developed the active ingredient. J.S. provided skin samples used to perform *in vitro* and some of the *ex vivo* studies. M.M. and A.S. designed the *in vitro* and *ex vivo* research studies. E.C. and L.L. conducted the clinical studies. M.M., A.S., E.C., and L.L. analyzed the data. R.R. was responsible of all the steps in this product development. M.M. and A.S. wrote the paper.

ETHICAL APPROVAL

All procedures performed in studies involving human participants were in accordance with the ethical standards of the institutional and/or national research committee and with the 1964 Helsinki declaration and its later amendments or comparable ethical standards.

DATA AVAILABILITY STATEMENT

The data that support the findings of this study are available from the corresponding author upon reasonable request.

ORCID

Marie Meunier  <https://orcid.org/0000-0003-2925-9094>

REFERENCES

- Wong R, Geyer S, Weninger W, Guimberteau JC, Wong JK. The dynamic anatomy and patterning of skin. *Exp Dermatol*. 2016;25:92-98.
- Fuchs E. Skin stem cells: rising to the surface. *J Cell Biol*. 2008;180:273-284.
- Martin MT, Vulin A, Hendry JH. Human epidermal stem cells: role in adverse skin reactions and carcinogenesis from radiation. *Mutat Res*. 2016;20.
- Pullar J, Carr A, Vissers M. The roles of vitamin C in skin health. *Nutrients*. 2017;9:866.
- Rippa AL, Kalabusheva EP, Vorotelyak EA. Regeneration of dermis: scarring and cells involved. *Cells*. 2019;8:607.
- Naylor EC, Watson REB, Sherratt MJ. Molecular aspects of skin ageing. *Maturitas*. 2011;69:249-256.
- Alves R, Ferreira L, Vale E, Bordalo O. Pseudoxanthoma elasticum papillary dermal elastolysis: a case report. *Dermatol Res Pract*. 2010;2010:1-4.
- Fenner J, Clark RAF. Anatomy, physiology, histology, and immunohistochemistry of human skin. In: *Skin Tissue Engineering and Regenerative Medicine*. Amsterdam: Elsevier; 2016:1-17.
- Wenstrup RJ, Florer JB, Brunskill EW, Bell SM, Chervoneva I, Birk DE. Type V collagen controls the initiation of collagen fibril assembly. *J Biol Chem*. 2004;279:53331-53337.
- Basisty N, Holtz A, Schilling B. Accumulation of "Old Proteins" and the critical need for MS-based protein turnover measurements in aging and longevity. *Proteomics*. 2020;20:1800403.
- Li Y, Lei D, Swindell WR, et al. Age-associated increase in skin fibroblast-derived prostaglandin E2 contributes to reduced collagen levels in elderly human skin. *J Invest Dermatol*. 2015;135:2181-2188.
- Varani J, Dame MK, Rittie L, et al. Decreased collagen production in chronologically aged skin. *Am J Pathol*. 2006;168:1861-1868.
- Shin J-W, Kwon S-H, Choi J-Y, et al. Molecular mechanisms of dermal aging and antiaging approaches. *IJMS*. 2019;20:2126.
- Quan T, Fisher GJ. Role of age-associated alterations of the dermal extracellular matrix microenvironment in human skin aging: a mini-review. *Gerontology*. 2015;61:427-434.
- Krutmann J, Bouloc A, Sore G, Bernard BA, Passeron T. The skin aging exposome. *J Dermatol Sci*. 2017;85:152-161.
- Silva SAME, Michniak-Kohn B, Leonardi GR. An overview about oxidation in clinical practice of skin aging. *An Bras Dermatol*. 2017;92:367-374.
- Dong KK, Damaghi N, Picart SD, et al. UV-induced DNA damage initiates release of MMP-1 in human skin. *Exp Dermatol*. 2008;17:1037-1044.
- Rodrigues Neves C, Gibbs S. Progress on reconstructed human skin models for allergy research and identifying contact sensitizers. In: Bagnoli F, Rappuoli R, (eds) *Three Dimensional Human Organotypic Models for Biomedical Research*. Springer International Publishing, 2021:103-129.
- Valacchi G, Pagnin E, Okamoto T, et al. Induction of stress proteins and MMP-9 by 0.8 ppm of ozone in murine skin. *Biochem Biophys Res Comm*. 2003;305:741-746.
- Philips N, Auler S, Hugo R, Gonzalez S. Beneficial regulation of matrix metalloproteinases for skin health. *Enzyme Res*. 2011;2011:1-4.
- Papakonstantinou E, Roth M, Karakiulakis G. Hyaluronic acid: a key molecule in skin aging. *Dermato-Endocrinol*. 2012;4:253-258.
- Gariboldi S, Palazzo M, Zanobbio L, et al. Low molecular weight hyaluronic acid increases the self-defense of skin epithelium by induction of α -Defensin 2 via TLR2 and TLR4. *J Immunol*. 2008;181(3):2103-2110.
- Essendoubi M, Gobinet C, Reynaud R, Angiboust JF, Manfait M, Piot O. Human skin penetration of hyaluronic acid of different molecular weights as probed by Raman spectroscopy. *Skin Res Technol*. 2016;22:55-62.
- Murakami T, Otsuki S, Okamoto Y, et al. Hyaluronic acid promotes proliferation and migration of human meniscus cells via a CD44-dependent mechanism. *Connect Tissue Res*. 2019;60:117-127.
- Wang X, Shu X, Li Z, et al. Comparison of two kinds of skin imaging analysis software: VISIA[®] from Canfield and IPP[®] from Media Cybernetics. *Skin Res Technol*. 2018;24:379-385.
- Holcomb JD. Helium plasma dermal resurfacing: VISIA CR assessment of facial spots, pores, and wrinkles—Preliminary findings. *J Cosmet Dermatol*. 2021;20:1668-1678.
- Goldsberry A, Hanke CW, Hanke KE. VISIA system: a possible tool in the cosmetic practice. *J Drugs Dermatol*. 2014;13:3.
- Lee DH, Oh J-H, Chung JH. Glycosaminoglycan and proteoglycan in skin aging. *J Dermatol Sci*. 2016;83:174-181.
- Zhong SP, Campoccia D, Doherty PJ, Williams RI, Benedetti L, Williams DF. Biodegradation of hyaluronic acid derivatives by hyaluronidase. *Biomaterials*. 1994;15:359-365.
- Campisi J. The biology of replicative senescence. *Eur J Cancer*. 1997;33:703-709.
- Furukawa A, Tada-Oikawa S, Kawanishi S, Oikawa S. H₂O₂ accelerates cellular senescence by accumulation of acetylated p53 via decrease in the function of SIRT1 by NAD⁺ depletion. *Cell Physiol Biochem*. 2007;20:45-54.
- Dasgupta J, Kar S, Liu R, et al. Reactive oxygen species control senescence-associated matrix metalloproteinase-1 through c-Jun-N-terminal kinase. *J Cell Physiol*. 2010;225:52-62.
- Ra H-J, Parks WC. Control of matrix metalloproteinase catalytic activity. *Matrix Biol*. 2007;26:587-596.
- Zegarska B, Pietkun K, Zegarski W, et al. Air pollution, UV irradiation and skin carcinogenesis: what we know, where we stand and what is likely to happen in the future? *Postepy Dermatol Alergol*. 2017;1:6-14.
- Fortino V, Maioli E, Torricelli C, Davis P, Valacchi G. Cutaneous MMPs are differently modulated by environmental stressors in old and young mice. *Toxicol Lett*. 2007;173:73-79.
- Flament F, Pierre J, Delhommeau K, Adam AS. How a working day-induced-tiredness may alter some facial signs in differently-aged Caucasian women. *Int J Cosmet Sci*. 2017;39:467-475.

How to cite this article: Meunier M, Scandolera A, Chapuis E, et al. The anti-wrinkles properties of sodium acetylated hyaluronate. *J Cosmet Dermatol*. 2022;21:2749-2762. <https://doi.org/10.1111/jocd.14539>